SEISMIC DECONVOLUTION USING ITERATIVE TRANSFORM-DOMAIN SPARSE INVERSION

MIN BAI and JUAN WU

School of Resources and Environment, North China University of Water Resources and Electric Power, Zhengzhou 450045, P.R. China. baimin@ncwu.edu.cn

ABSTRACT

Bai, M. and Wu, J., 2018. Seismic deconvolution using iterative transform-domain sparse inversion. *Journal of Seismic Exploration*, 27: 103-116.

Post-stack seismic deconvolution is a classic inverse problem in seismic exploration, which can tremendously improve the resolution of seismic reflectors. Because of the ill-posedness of deconvolution, there ha[illegible]h problem by applying different constraints. We propose to apply a transform-domain sparsity constraint to the inverse deconvolution problem and propose to solve it by a simple iterative thresholding algorithm. Compared with the alternative Wiener filtering, the proposed iterative transform-domain thresholding algorithm can improve the signal-to-noise ratio (SNR) and the spatial coherency of the seismic data after deconvolution. Both synthetic and field data example are used to demonstrate the superior performance of the proposed algorithm.

KEY WORDS: seismic deconvolution, sparse inversion, sparse constraint, noise attenuation, thresholding operator.

INTRODUCTION

The successful characterization of subsurface hydrocarbon reservoirs from seismic data highly depends on a clean and high-resolution seismic image. A lot of methods have been developed to improve the quality of seismic images. One widely used approach to improve seismic image is to apply some random noise attenuation approaches to remove the noise (either

0963-0651/18/$5.00

generated from the migration artifacts or from the ambient noise on the raw pre-stack seismic data) (Liu et al., 2016e,b,c; Kong et al., 2016; Wu et al., 2016; Siahsar et al., 2017a,c). The prediction based denoising approach (Canales, 1984; Liu et al., 2012), statistics-based denoising approach (Gan et al., 2016c; Chen et al., 2017b), eigen-image based denoising approach (Huang et al., 2016; Xue et al., 2016; Huang et al., 2017a,b; Chen et al., 2017c; Zhang et al., 2017), morphological operation based methods (Li et al., 2016a,b; Huang et al., 2017c), inversion based methods (Zu et al., 2017a), dictionary learn- ing based methods (Siahsar et al., 2017b; Chen, 2017), and transform-domain thresholding based denoising approaches (Fomel and Liu, 2010; Gan et al., 2016a; Zu et al., 2016a; Sun and Wang, 2016; Gan et al., 2016b; Zhang et al., 2016; Xue et al., 2017) are the four main denoising approaches existing in the seismic data processing community (Liu et al., 2012; Chen and Fomel, 2015; Chen, 2015; Yang et al., 2015). All the published methods have their own pros and cons regarding the denoising assumptions. However, none of the existing de- noising methods consider increasing the resolution together with denoising simultaneously.

Increasing the resolution of seismic data is usually a separate processing step by deconvolution (Liu et al., 2016a). In this paper, we propose a novel framework in which the noise attenuation problem and the resolution enhancing problem are solved simultaneously. We first review the convolution model widely used in the traditional seismic deconvolution literature and then compare the traditional Wiener filtering method and sparsity promoting method in the context of optimization. Then, we further introduce the proposed mathematical model and point the key difference between the proposed method and traditional alternatives. The new optimization problem is solved using an iterative framework with a simple FK thresholding as a constraining operator. The principal advantage of the pro- posed method is that it takes advantage of the spatial coherency of post-stack seismic data and is able to increase the resolution while rejecting the random noise simultaneously. The proposed algorithm framework is based on the well-known convolution model and can be applied in any 2D or 3D post-stack seismic data. The sparse constraint is not limited to the FK thresholding operator. The application of other sparsity-promoting transforms is straightforward and the comparison of the performance of different methods is worth being investigated. Both synthetic and field data examples show very successful performance of the proposed approach.

THEORY

Let us start the theory from the basic convolution model, which assumes the observed trace d is the result of the convolution of the wavelet w with the reflectivity series r plus some superposed noise n:

$$d(t) = w(t) * r(t) + n(t) \quad , \tag{1}$$

where $*$ denotes convolution.

We can write eq. (1) in the matrix-vector form:

$$\mathbf{d} = \mathbf{W}\mathbf{r} + \mathbf{n} \quad . \tag{2}$$

For the multi-channel case, **d**, **r**, and **n** are all vectorized matrices. **W** is a block diagonal matrix.

Seismic deconvolution aims to solve eq. (2) for **r**. Because **W** is highly singular and **n** is unknown, eq. (2) is highly under-determined. In order to solve the problem, we need to add some constraints. With different constraints, problem (2) can be transferred into different alternative minimization problems:

1. With a least-energy constraint on the reflectivity:

$$\min_{\mathbf{r}} \frac{1}{2} \| \mathbf{d} - \mathbf{W}\mathbf{r} \|_2^2 + \epsilon \| \mathbf{r} \|_2^2 \quad , \tag{3}$$

2. With a sparsity constraint on the reflectivity.

$$\min_{\mathbf{r}} \frac{1}{2} \| \mathbf{d} - \mathbf{W}\mathbf{r} \|_2^2 + \epsilon \| \mathbf{r} \|_1 \quad . \tag{4}$$

Here, $\| \cdot \|_2$, $\| \cdot \|_1$ denote L_2 and L_1 norms, respectively. ε is a controlling factor. Eq. (3) also refers to the Wiener deconvolution, while eq. (4) refers to the sparse deconvolution. The solution of eq. (3) can be obtained by

$$\hat{\mathbf{r}}_{LS} = (\mathbf{W}^H\mathbf{W} + \epsilon\mathbf{I})^{-1}\mathbf{W}^H\mathbf{d} \quad , \tag{5}$$

where $\hat{r}_{LS}$ is the solution using the least-squares criterion (5), $[\cdot]^H$ denotes adjoint. Eq. (4) can be solved using a iterative thresholding algorithm (Chen et al., 2015; Gan et al., 2015; Liu et al., 2016d; Zu et al., 2016b; Zhou, 2017):

$$\mathbf{r}_{n+1} = \mathbf{T}_\alpha(\mathbf{r}_n + \lambda\mathbf{W}^H(\mathbf{d} - \mathbf{W}\mathbf{r}_n)) \quad , \tag{6}$$

where T_α is a thresholding operator with a input parameter α. λ is the update step size. The thresholding operator T_α can be chosen as a soft thresholding operator:

$$\mathbf{T}_\alpha^s(x) = \begin{cases} (|x| - \alpha) * sign(x) & \text{for} \quad |x| \geq \alpha \\ 0 & \text{for} \quad |x| < \alpha \end{cases} , \tag{7}$$

or as a hard thresholding operator:

$$\mathbf{T}_\alpha^h(x) = \begin{cases} x & \text{for} \quad |x| \geq \alpha \\ 0 & \text{for} \quad |x| < \alpha \end{cases} . \tag{8}$$

In this paper, we propose a different sparsity constraint. Instead of enforcing the sparsity constraint directly on the reflectivity, we propose to enforce the sparsity constraint on the transform-domain coefficients of the reflectivity.

$$\min_{\mathbf{r}} \frac{1}{2} \| \mathbf{d} - \mathbf{W}\mathbf{r} \|_2^2 + \epsilon \| \mathbf{A}\mathbf{r} \|_1 . \tag{9}$$

Here, $\mathbf{A}$ denotes a sparsity-promoting transform. Note that $\mathbf{Ar}$ denotes both the product of $\mathbf{A}$ and $\mathbf{r}$ and the transform of $\mathbf{r}$. Here, we assume $\mathbf{A}$ is a linear transform, and the transform of $\mathbf{r}$ is equal to the product of matrix $\mathbf{A}$ and vector $\mathbf{r}$. In order to solve eq. (9), we can use a similar iterative algorithm as (6):

$$\mathbf{r}_{n+1} = \mathbf{A}^{-1}\mathbf{T}_\alpha\mathbf{A}(\mathbf{r}_n + \lambda\mathbf{W}^H(\mathbf{d} - \mathbf{W}\mathbf{r}_n)) , \tag{10}$$

where $\mathbf{A}^{-1}$ is the inverse sparsity-promoting transform. In this paper, we choose the simple Fourier transform as the sparsity-promoting transform.

EXAMPLES

In order to numerically evaluate the performance of inverted reflectivity model, we define the following signal-to-noise ratio (SNR) (Chen and Ma, 2014; Zu et al., 2016b; Chen, 2016)

$$SNR_n = 10\log_{10}\frac{\|\mathbf{r}\|_2^2}{\|\mathbf{r} - \mathbf{r}_n\|_2^2} , \tag{11}$$

where $\mathbf{r}$ is the true reflectivity. $\mathbf{r}_n$ is the inverted model after the n-th iteration.

The first example is shown in Figs. 1-7. Fig. 1a shows the exact reflectivity model, which is a band-limited reflectivity model, and Fig. 1b shows the observed post-stack data. Fig. 2a shows the result using the proposed iterative sparse inversion method after 100 iterations. Fig. 2b shows the result from the traditional Wiener filtering. The resolution of the reflectivity image in Fig. 2a is higher than the resolution of Fig. 2b, but the comparison is not very obvious. To compare in a more salient way, we plot the error sections in Fig. 3. The error sections here mean the difference sections between the exact solution and the inverted model. It is quite clear that the error using the sparse inversion method is almost negligible while the error using the Wiener filtering method is very large, which proves the correctness of the proposed iterative algorithm in solving the inverse problem. To make the comparison even clearer, we show some results in the greyscale plots (Fig. 4). Fig. 5 shows the comparison of the reflectivity images using the proposed and the traditional Wiener filtering methods. In the greyscale plot, the comparison is very clear that the proposed method obtains a high-resolution result while the Wiener filtering method causes some side-lobes of the waveforms which degrade the resolution a lot. The side-lobes are caused due to the large stability factor used in the traditional Wiener filtering method. Fig. 5 shows the error sections of two methods in greyscale plots. The comparison further shows that the proposed method can obtain very accurate inversion result. In this paper, we use a percentile strategy to choose the optimal threshold value (Chen et al., 2014). More specifically, we preserve a percentage of the largest coefficients (2%) in the transform domain. The step size will affect the convergence rate and stability. If we choose a very large step size, the iterations are dangerous, which means they may not converge. In this paper, we choose 0.5 to obtain the presented results. In the Wiener filtering method, we use 1% of the largest value of spectrum coefficients as the stability factor.

To show how the result evolve during the iterations, we plot three models (after 5, 20, and 80 iterations, respectively) during inversion, and their corresponding predicted data, in Fig. 6. The results during iterations show that the model gets closer and closer to the exact solution shown in Fig. 1a and the data misfit is becoming smaller and smaller during the inversion. Fig. 7 shows the SNRs of the inverted model during the 100 iterations. The SNR goes from 2.173 dB in the beginning to 33.5 dB in the final result. As a comparison, we also calculate the SNR of the Wiener filtering method, which is 16.78 dB. The SNR comparison provides a quantitative measure of the relative performance between Wiener filtering and the proposed method in this example.

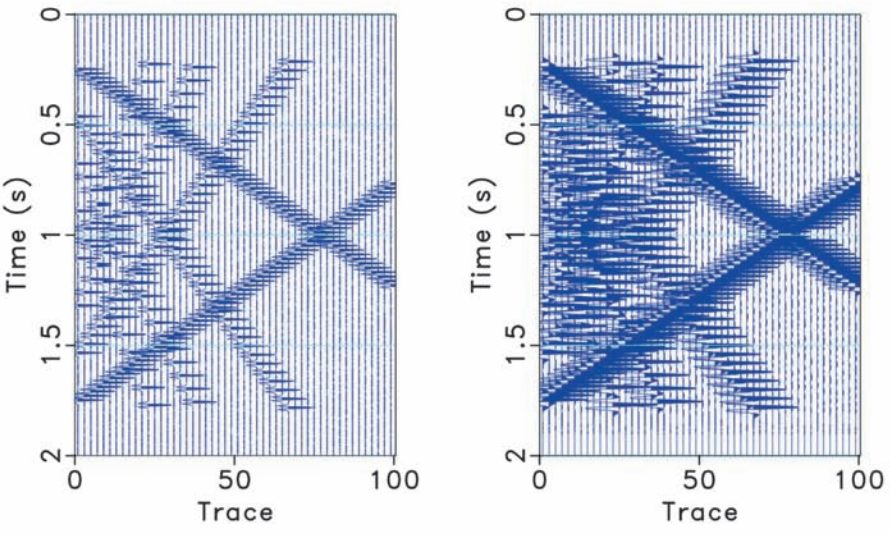

Fig. 1. (a) Reflectivity. (b) Observed data.

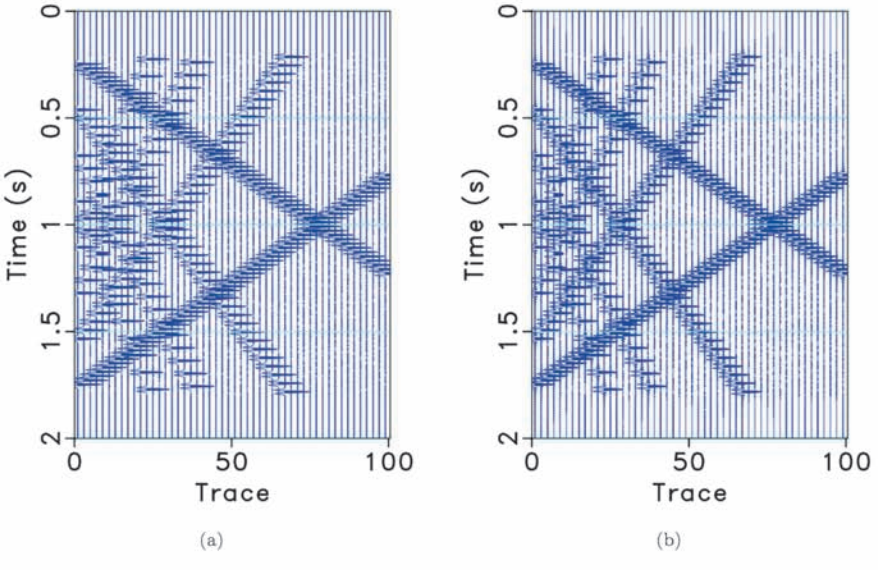

Fig. 2. (a) Inverted reflectivity using sparse inversion. (b) Inverted reflectivity using Wiener filtering.

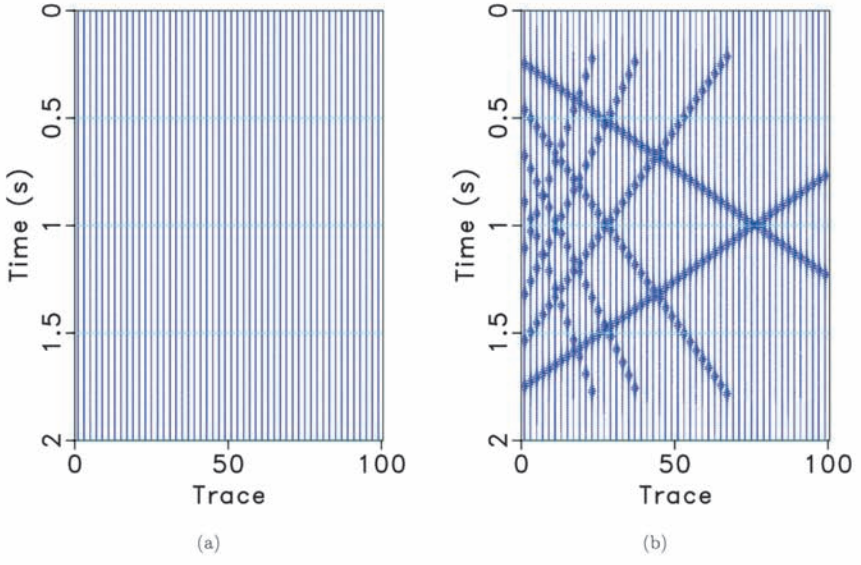

Fig. 3. Error section. (a) Inverted reflectivity using sparse inversion. (b) Inverted reflectivity using Wiener filtering.

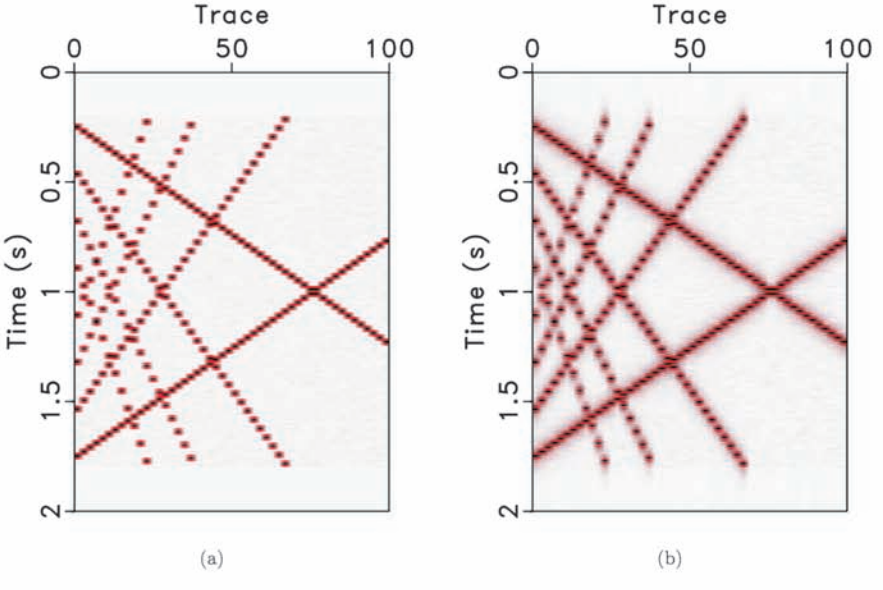

Fig. 4. Greyscale comparison. (a) Error section using sparse inversion. (b) Error section using Wiener filtering.

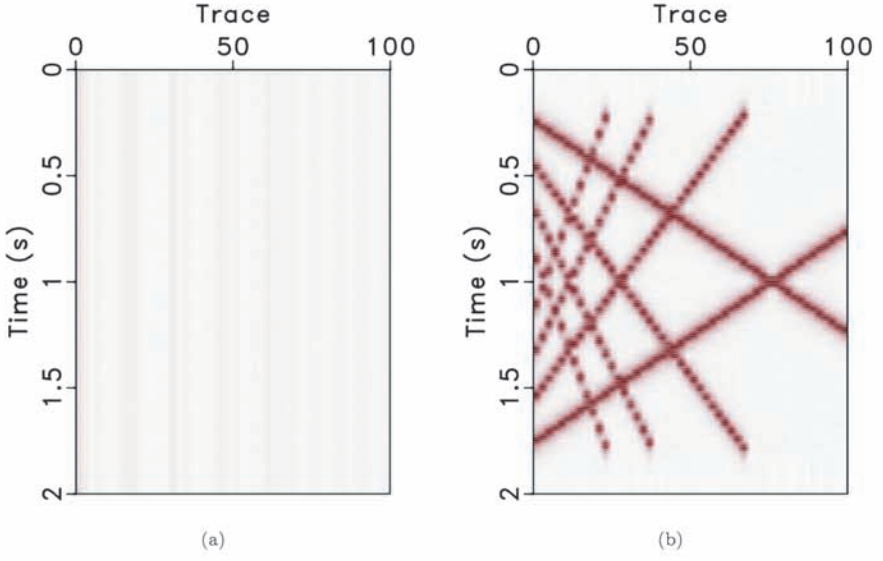

Fig. 5. Greyscale comparison. (a) Inverted reflectivity using sparse inversion. (b) Inverted reflectivity using Wiener filtering.

We then apply the proposed method to a real post-stack seismic data. Fig. 8a shows the very noisy and low-resolution field data from a land survey in China. Fig. 8b shows the final deconvolved result using the sparse inversion method and Fig. 8c shows the result using the Wiener filtering method. In this example, we use 200 iterations to obtain the result. In the transform domain, we preserve 5% of the largest coefficients. We use the same stability factor selection method as the synthetic example. It is very clear that the proposed sparse inversion method obtains a much improved image by enhancing the resolution and increasing the SNR of the data. Here, SNR is roughly evaluated by human visualization. The Wiener filtering method, although gets some improvement, has lower resolution and more residual noise than the proposed method.

In the presented examples, it has been shown that if the reflectivity models satisfy the ”sparsity” assumption in some transform domains, the sparse inversion based method can obtain a significantly cleaner result than that from the traditional Wiener filtering method. However, if the ”sparsity” assumption is not satisfied, e.g., when the earth reflectivity is dense, the Wiener filtering method can still outperform the sparse inversion method, with the compromise of introducing some unwanted noise. Our initial guess of which method to use in practice is that if the seismic data shows obvious spatial coherency, which means the transform domain can be sparse, we should use the sparse inversion method. While the seismic data contains

obvious spatial discontinuities, we suggest using the Wiener filtering method as the common routine. However, our guess requires future validation through more comprehensive numerical and field tests. In many seismic exploration settings, lateral resolution can be very important (Chen et al., 2017a). Regarding the lateral resolution, because the sparsity based method takes advantage of spatial coherence for regularizing the reflectivity model, the spatial resolution may be decreased to some extent, which also results in a slightly higher uncertainty about the lateral resolution. The traditional Wiener filtering method, however, due to its trace-by-trace processing nature, the spatial resolution can be preserved well. The proposed method and traditional Wiener filtering method should not vary much regarding the vertical resolution (Chen and Jin, 2015; Zu et al., 2017b).

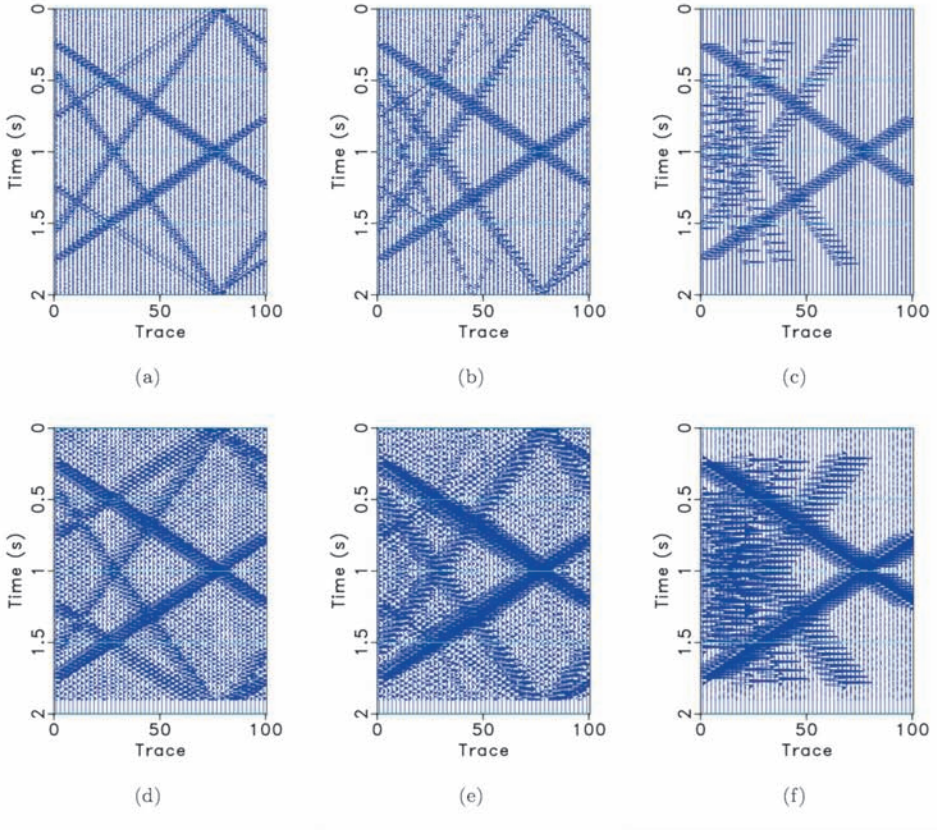

Fig. 6. Inversion results and the forward modeled results during the iteration (each column correspond to r_n and Wr_n in eq. (10) for a specific n). (a) 5 iteration (SNR=0.57dB). (b) 20 iteration (SNR = 2.69 dB). (c) 80 iteration (SNR = 25.63 dB). (d) Forward modeled result using (a). (e) Forward modeled result using (b). (f) Forward modeled result using (c).

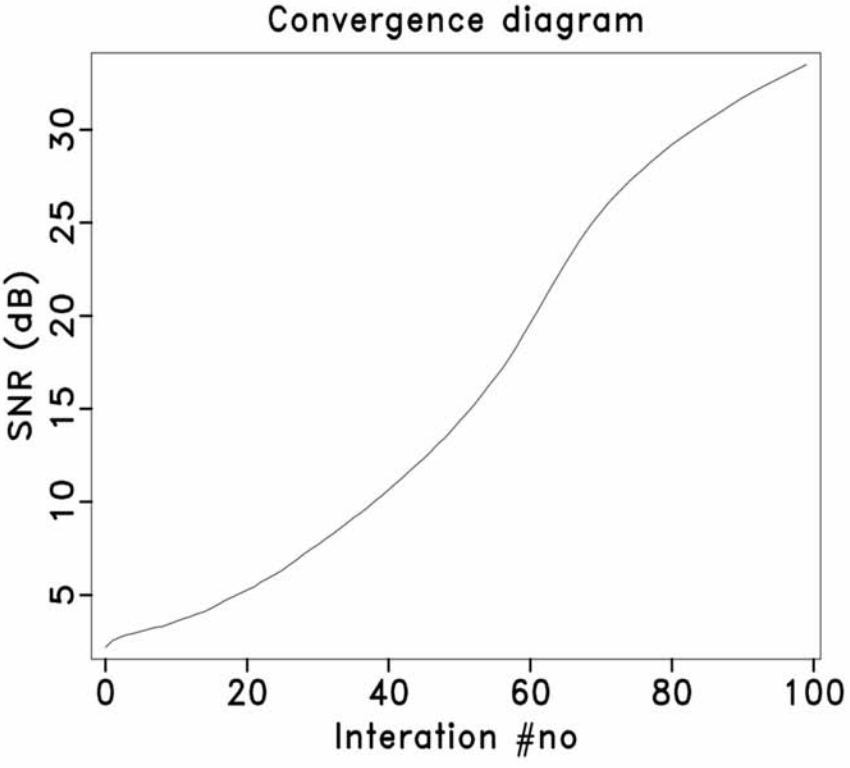

Fig. 7. Convergence diagram of the signal-to-noise ratio.

CONCLUSIONS

Improving the resolution while decreasing the ambient random noise in post-stack images is a vital step in seismic data processing. The traditional Wiener filtering method that is based on least-squares inversion is capable of improving the data quality to some extent but will still cause very strong noise due to the stabilization. We propose a very effective sparse inversion method for deconvolving the post-stack seismic data using a thresholding operator in a sparse transform domain as a constraint. Results show that the proposed method can obtain very high-resolution reflectivity image and can remove the spatially incoherent random noise thanks to the sparsity-promoting thresholding operator. Both synthetic and field data examples confirm the validity and effectiveness of the proposed algorithm framework.

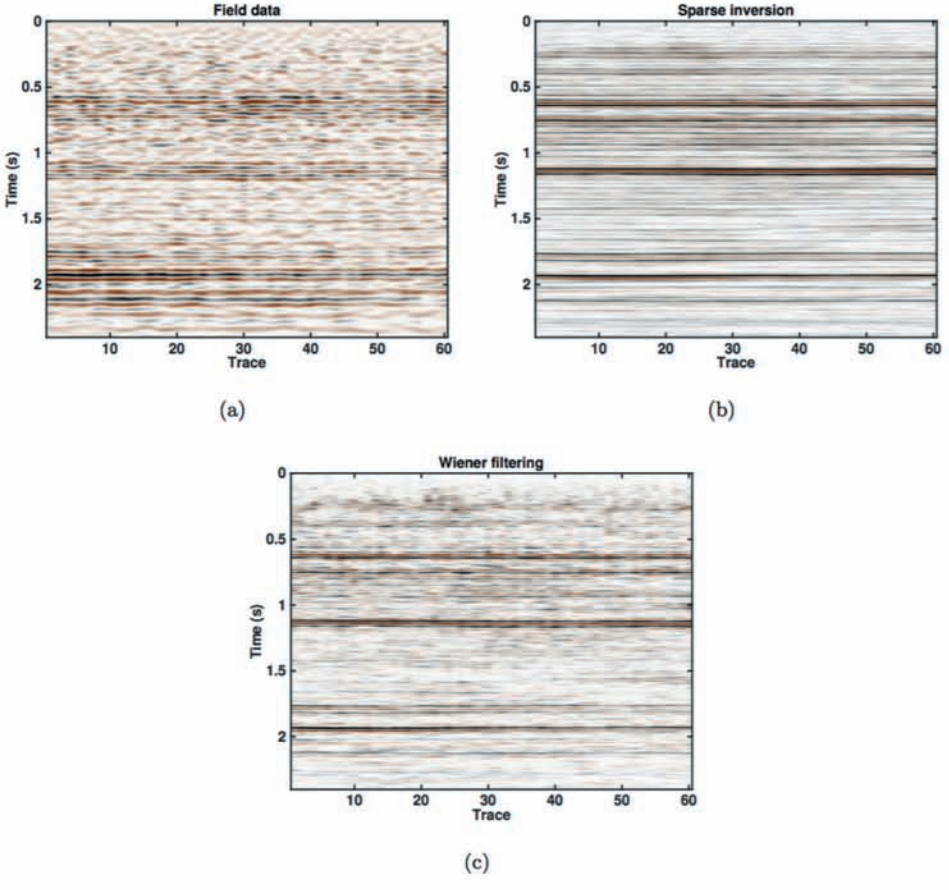

Fig. 8. Field data example. (a) Post-stack field data. (b) Inverted reflectivity using the proposed sparse inversion method. (b) Inverted reflectivity using Wiener filtering method.

ACKNOWLEDGEMENTS

The project is supported by the National Natural Science Foundation of China (Grant No. 41704121) and the starting fund at North China University of Water Resources and Electric Power.
(Grants No. 201705002, 201705003).

REFERENCES

Canales, L., 1984. Random noise reduction. Expanded Abstr., 54th Ann. Internat. SEG Mtg., Atlanta: 525–527.

Chen, G., Fu, L.Y., Chen, K.F., Sun, W., Wei, W. and Guan, X., 2017a. Calculation of the seismic imaging complexity of complex geological structures. J. Seismic Explor., 26: 81–104.

Chen, W., Yuan, J., Chen, Y. and Gan, S., 2017b. Preparing the initial model for iterative deblending by median filtering. J. Seismic Explor., 26: 25–47.

Chen, Y., 2015. Iterative deblending with multiple constraints based on shaping regularization. IEEE Geosci. Remote Sens. Lett., 12: 2247–2251.

Chen, Y., 2016. Dip-separated structural filtering using seislet thresholding and adaptive empirical mode decomposition based dip filter. Geophys. J. Internat., 206: 457–469.

Chen, Y., 2017. Fast dictionary learning for noise attenuation of multidimensional seismic data. Geophys. J. Internat., 209: 21–31.

Chen, Y. and Fomel, S., 2015. Random noise attenuation using local signal-and-noise orthogonalization. Geophysics, 80(6): WD1–WD9.

Chen, Y., Fomel, S. and Hu, J., 2014. Iterative deblending of simultaneous-source seismic data using seislet-domain shaping regularization. Geophysics, 79: V179–V189.

Chen, Y., Gan, S., Qu, S. and Zu, S., 2015. Sparse inversion for water bubble removal and spectral enhancement. J. Appl. Geophys., 117: 81–90.

Chen, Y. and Jin, Z., 2015. Simultaneously removing noise and increasing resolution of seismic data using waveform shaping. IEEE Geosci. Remote Sens. Lett., 13: 102-104.

Chen, Y. and Ma, J., 2014. Random noise attenuation by f-x empirical mode decomposition predictive filtering. Geophysics, 79: V81–V91.

Chen, Y., Zhou, Y., Chen, W., Zu, S., Huang, W. and Zhang, D., 2017c. Empirical low rank decomposition for seismic noise attenuation. IEEE Transact. Geosci. Remote Sens., 55: 4696–4711.

Fomel, S. and Liu, Y., 2010,. Seislet transform and seislet frame. Geophysics, 75: V25-V38.

Gan, S., Chen, Y., Wang, S., Chen, X., Huang, W. and Chen, H., 2016a. Compressive sensing for seismic data reconstruction using a fast projection onto convex sets algorithm based on the seislet transform. J. Appl. Geophys., 130: 194-208.

Gan, S., Wang, S., Chen, Y. and Chen, X., 2016b. Simultaneous-source separation using iterative seislet-frame thresholding. IEEE Geosci. Remote Sens. Lett., 13: 197-201.

Gan, S., Wang, S., Chen, Y., Chen, X. and Xiang, K., 2016c. Separation of simultaneous sources using a structural-oriented median filter in the flattened dimension. Comput. Geosci., 86: 46-54.

Gan, S., Wang, S., Chen, Y., Zhang, Y. and Jin, Z., 2015. Dealiased seismic data interpolation using seislet transform with low-frequency constraint. IEEE Geosci. Remote Sens. Lett., 12: 2150-2154.

Huang, W., Wang, R., Chen, X. and Chen, Y., 2017a. Double least squares projections method for signal estimation. IEEE Transact. Geosci. Remote Sens., 55: 4111-4129.

Huang, W., Wang, R., Chen, Y., Li, H. and Gan, S., 2016. Damped multichannel singular spectrum analysis for 3D random noise attenuation. Geophysics, 81(4): V261–V270.

Huang, W., Wang, R., Yuan, Y., Gan, S. and Chen, Y., 2017b. Signal extraction using randomized-order multichannel singular spectrum analysis. Geophysics, 82(2): V59-V74.

Huang, W., Wang, R., Zhang, D., Zhou, Y., Yang, W. and Chen, Y., 2017c. Mathematical morphological filtering in a rotating coordinate system for coherent noise attenuation. Geophysics, 82: V369-V384. doi: 10.1190/geo2016–0580.1.

Kong, D., Peng, Z., He, Y. and Fan, H., 2016. Seismic random noise attenuation using directional total variation in the shearlet domain. J. Seismic Explor., 25: 321-338.

Li, H., Wang, R., Cao, S., Chen, Y. and Huang, W., 2016a. A method for low-frequency noise suppression based on mathematical morphology in microseismic monitoring. Geophysics, 81(3): V159–V167.

Li, H., Wang, R., Cao, S., Chen, Y., Tian, N. and Chen, X., 2016b. Weak signal detection using multiscale morphology in microseismic monitoring. J. Appl. Geophys., 133: 39–49.

Liu, C., Wang, D., Hu, B. and Wang, T., 2016a. Seismic deconvolution with shearlet sparsity constrained inversion. J. Seismic Explor., 25: 433-445.

Liu, G., Chen, X., Du, J. and Wu, K., 2012. Random noise attenuation using f-x regularized nonstationary autoregression. Geophysics, 77: V61-V69.

Liu, W., Cao, S. and Chen, Y., 2016b. Applications of variational mode decomposition in seismic time-frequency analysis. Geophysics, 81(5): V365-V378.

Liu, W., Cao, S., Chen, Y. and Zu, S., 2016c. An effective approach to attenuate random noise based on compressive sensing and curvelet transform. J. Geophys. Engineer., 13: 135-145.

Liu, W., Cao, S., Gan, S., Chen, Y., Zu, S. and Jin, Z., 2016d. One-step slope estimation for dealiased seismic data reconstruction via iterative seislet thresholding. IEEE Geosci. Remote Sens. Lett., 13: 1462-1466.

Liu, W., Cao, S., Liu, Y. and Chen, Y., 2016e. Synchrosqueezing transform and its applications in seismic data analysis. J. Seismic Explor., 25: 27-44.

Siahsar, M.A.N., Abolghasemi, V. and Chen, Y., 2017a. Simultaneous denoising and interpolation of 2D seismic data using data-driven non-negative dictionary learning. Sign. Process., 141: 309-321.

Siahsar, M.A.N., Gholtashi, S., Kahoo, A.R., Chen, W. and Chen, Y., 2017b. Data-driven multi-task sparse dictionary learning for noise attenuation of 3D seismic data. Geophysics, 82(6): V385-V396. doi: 10.1190/geo2017-0084.1.

Siahsar, M.A.N., Gholtashi, S., Olyaei, E., Chen, W. and Chen, Y., 2017c. Simultaneous denoising and interpolation of 3D seismic data via damped data-driven optimal singular value shrinkage. IEEE Geosci. Remote Sens. Lett., 14: 1086-1090.

Sun, W. and Wang, H., 2016. Water-layer-related demultiple method using constraints in the sparse, local tau-p domain. J. Seismic Explor., 25: 463–483.

Wu, J., Wang, R., Chen, Y., Zhang, Y., Gan, S. and Zhou, C., 2016. Multiples attenuation using shaping regularization with seislet domain sparsity constraint. J. Seismic Explor., 25: 1-9.

Xue, Y., Chang, F., Zhang, D. and Chen, Y., 2016. Simultaneous sources separation via an iterative rank-increasing method. IEEE Geosci. Remote Sens. Lett., 13: 1915-1919.

Xue, Y., Man, M., Zu, S., Chang, F. and Chen, Y., 2017. Amplitude-preserving iterative deblending of simultaneous source seismic data using high-order radon transform. J. Appl. Geophys., 139: 79-90.

Yang, W., Wang, R., Wu, J., Chen, Y., Gan, S. and Zhong, W., 2015. An efficient and effective common reflection surface stacking approach using local similarity and plane-wave flattening. J. Appl. Geophys., 117: 67-72.